Algorithmic complexity of EEG as a prognosis biomarker of neurodegeneration in idiopathic rapid eye movement behavior disorder (RBD)

Giulio Ruffini[a,b,*], David Ibañez[a], Eleni Kroupi[a], Jean-François Gagnon[c,e], Jacques Montplaisir[c,f], Ronald B. Postuma[c,d], Marta Castellano[a], Aureli Soria-Frisch[a]

[a]*Starlab Barcelona, Avda. Tibidabo, 47bis, 08035 Barcelona, Spain*
[b]*Neuroelectrics Corporation, 210 Broadway, Cambridge, MA 02139, USA*
[c]*Centre for Advanced Research in Sleep Medicine, Hôpital du Sacré-Cœur de Montréal, Montreal, Canada*
[d]*Department of Neurology, Montreal General Hospital, Montreal, Canada*
[e]*Department of Psychology, Université du Québec à Montréal, Montreal, Canada*
[f]*Department of Psychiatry, Universit 'e de Montréal*

Abstract

Rapid eye movement sleep (REM) behavior disorder (RBD) is a serious risk factor for neurodegenerative diseases such as Parkinson's disease (PD). We describe here the analysis of resting state EEG data collected from idiopathic RBD patients and healthy controls (HC) forming a balanced cohort of 178 subjects in which a subset of RBD patients eventually developed either PD or dementia with Lewy bodies (DLB). In earlier work [1, 2], we implemented support vector machine classifiers using EEG mean spectral features to predict the course of disease with an AUC of 85% in several classification problems, and, later, in [3] an Echo State recurrent neural network that delivered high classification accuracy on balanced datasets. Here we investigate the data in a complementary way and describe the statistics of global algorithmic complexity of these EEG multi-channel time series, which are analyzed as spectrograms (time-frequency plots). We provide an upper bound to algorithmic complexity using Lempel-Ziv-Welch compression (LZW) and entropy rate of the set of stacked spectrograms of 14 channels for each subject. Both LZW and entropy rate highlight strong

*Corresponding author, giulio.ruffini@neuroelectrics.com

statistically significant differences between the groups. Results are compared to those using the well-known ratio of fast to slow frequency power associated with slowing of EEG [4, 5], which they are seen to complement by picking up dynamical features of EEG spectral series. Poor prognosis in RBD appears to be associated with decreased temporal variability of the EEG spectrum in beta and gamma frequencies.

Keywords: Biomarkers, EEG, LZW, PD, LBD

---

1. Introduction

The human brain can be modeled as a highly dimensional complex dynamical system which instantiates electrochemical communication and computation. Electroencephalographic (EEG) and magnetoencephalographic (MEG) signals contain rich information associated with these processes, and are accessible non-invasively. To a large extent, progress in the analysis of such signals has been driven by the study of classical temporal and spectral features in electrode space, and applied to the study the human brain in both health and disease. For example, the "slowing down" of EEG is known to characterize neurodegenerative diseases [6, 4], and the slow to fast ratio (the ratio of power in delta and theta bands to alpha and beta) has shown good discriminatory power [4, 5]. However, brain activity measurements exhibit non-linear dynamics and non-stationarity, limiting the usefulness of classical, linear approaches. The complexity of these signals calls for the use of novel methods capable of exploiting such features, representing rich spatio-temporal hierarchical structures. Interestingly, deep learning techniques in particular and neural networks in general are bio-inspired by the brain —the same biological system generating the electric signals we aim to decode. They should be well suited for the task. In past work we studied a particular class of recurrent neural networks (RNNs) called Echo State Networks (ESNs) that combine the power of RNNs for classification of temporal patterns and ease of training, reasoning that RNNs and, in particular, ESNs implement non-linear dynamics with memory and seem ideally poised for the classification

of complex time series data.

REM Behavior Disorder (RBD) is a serious risk factor for neurodegenerative diseases such as Parkinson's disease (PD). RBD is a parasomnia characterized by vivid dreaming and dream-enacting behaviors associated with REM sleep without muscle atonia [7]. Idiopathic RBD occurs in the absence of any neurological disease or other identified cause, is male-predominant and its clinical course is generally chronic progressive [8]. Several longitudinal studies conducted in sleep centers have shown that many patients diagnosed with the idiopathic form of RBD will eventually be diagnosed with a neurological disorder such as Parkinson disease (PD) and dementia with Lewy bodies (DLB) [9, 8, 7].

In a dataset of recordings of resting state EEG from idiopathic RBD patients (called henceforth RBD for data analysis) who later converted to Parkinson's disease (PD) and from healthy controls (HC), we showed that using such recurrent networks using temporal series of EEG power led to an accuracy of 85% in the binary, balanced classification problem of healthy controls versus PD patients [3]. The main limitations of using ESNs, in our view, were a) computational cost and b) the need for feature selection (e.g., which frequency bands and channels to use as inputs to feed the network).

Here we fall back to statistics to explore a different feature extracted from EEG data. We hypothesize that EEG algorithmic complexity decreases with PD's neurodegenerative disease progression, something already reported in the literature in Alzheimer's Disease [10, 11, 12]. Our assumption is that relevant aspects in EEG data are contained in compositional features in the time-frequency representation. As posited in [3, 3], such characteristics should be reflected by the algorithmic information content in the data, and they should reflect cognitive health and conscious state. Algorithmic information was formalized by the mathematical concept of algorithmic complexity or Kolmogorov complexity ($\mathcal{K}$), co-discovered during the second half of the 20th century by Solomonoff, Kolmogorov and Chaitin. We recall its definition: *the Kolmogorov complexity of a string is the length of the shortest program capable of generating it.* More precisely, let $\mathcal{U}$ be a universal computer (a TM), and let p be a program. Then

the Kolmogorov or algorithmic complexity of a string x with respect to $\mathcal{U}$ is given by $\mathcal{K}_{\mathcal{U}(x)} = \min_{p:\mathcal{U}(p)=x} l(p)$, i.e., the length $l(p)$ of the shortest program that prints the string x and then halts (see e.g., [13, 14]). Crucially, although the precise length of this program depends on the programming language used, it does so only up to a string-independent constant.

Algorithmic information is notoriously difficult to estimate. Here we analyze our hypothesis from the angle of complexity as measured from LZW and entropy rate, two related measures that provide an upper bound to algorithmic complexity.

Table 1: **Baseline sociodemographic and clinical data for the four groups.**

Group (N for F/M)	**HC (37/29)**	**RBD (18/68)**	**PD (5/8)**	**DLB (2/11)**
Mean age (yr)	66 ± 9	67 ± 7	67 ± 7	71 ± 6
Mean follow-up (yr)	1 ± 1	4 ± 3	4 ± 2	4 ± 2

Mean and standard deviation for age and follow up per group are provided (units are years). Acronyms: HC: healthy controls; RBD: idiopathic RBDs who remained idiopathic RBD on follow up; PD: idiopathic RBD who converted to PD on follow up; DLB: idiopathic RBD who converted to LBD on follow up. In parenthesis, gender breakdown of each group (N for female, male).

2. Materials and methods

2.1. Participants

Patients were recruited at the Center for Advanced Research in Sleep Medicine of the Hôpital du Sacrè-Cœur de Montral. All patients with full EEG montage for resting-state EEG recording at baseline and with at least one follow-up examination after the baseline visit were included in the study. The first valid EEG for each patient enrolled in the study was considered baseline. Participants

also underwent a complete neurological examination by a neurologist specialized in movement disorders and a cognitive assessment by a neuropsychologist. No controls reported abnormal motor activity during sleep or showed cognitive impairment on neuropsychological testing. The protocol was approved by the hospital's ethics committee, and all participants gave their written informed consent to participate. For mode details, see [4].

2.2. EEG dataset

As with previous work [15], the first level data in this study consisted of resting-state EEG collected from awake patients and healthy controls using 14 scalp electrodes. The recording protocol consisted of conditions with periods of "eyes open" of variable duration ($\sim$ 2 minutes) followed by periods of "eyes closed" in which patients were not asked to perform any particular task. EEG signals were digitized with 16 bit resolution at a sampling rate of 256 S/s. The amplification device implemented hardware band pass filtering between 0.3 and 100 Hz and notch filtering at 60 Hz to minimize the influence of power line noise. All recordings were referenced to linked ears.

After quality check and rejection of subjects with insufficient data, or rejection healthy subjects with abnormal cognition at the time of acquisition, the dataset includes a total of 178 patients who were diagnosed with idiopathic REM (random eye movement sleep) Behavioral Disorder (RBD) at the time of EEG acquisition and 66 healthy controls (HC) without sleep complaints in which RBD was excluded. EEG data was collected in every patient at baseline, i.e., when they were still diagnosed with idiopathic RBD. After 1-10 years of clinical follow-up, thirteen patients developed Parkinson disease (PD), thirteen Lewy body dementia (DLB) and the remaining eighty-six ones remained idiopathic RBD. Summary demographic data are provided in Table 1.

2.3. Complexity features

We will focus here on the concepts of description length and entropy rate. In order to provide an upper bound to description length or algorithmic complexity,

we will rely on Lempel-Ziv-Welch compression. The main idea in LZW is to look for repeating patterns in the data, and instead of rewriting a repeating sequences, refer to the last one seen [16]. After applying LZW to a string we end up with a set of words (or phrases, as they are sometimes called) $c(n)$ that go into a dictionary. The length of the compressed string will be $l_{LZW} \leq n$. We note that LZW can be used to obtain an upper bound on algorithmic complexity, but, given its reduced programming repertoire (LZW is the Kolmogorov complexity computed with a limited set of programs that only allow copy and insertion in strings [17]), it will fail to compress random-looking data generated by simple, but highly recursive programs, e.g., the sequence of binary digits of π, with more sophisticated regularities than sequence repetition (deep programs [18]). As an example of how LZW or entropy rate are limited tools for compression, and therefore poor cousins of algorithmic complexity, consider a string and its "time-reversed" version in a file with the ordering of symbols inverted, or a string and "time-dilated" string where each symbol is repeated, say 2 times. Such simple algorithmic manipulations will not be detected and exploited by LZW.

Let $H_0(p) = -p \log p - (1-p)\log(1-p)$ denote the univariate or zero order entropy, with p the probability of a Bernoulli (binary) process (Markov chain of order zero). By the entropy rate of the stochastic process $\{X_i\}$, we will mean

$$\mathcal{H}(X) = \lim_{n\to\infty} \frac{1}{n} H(X_1, ..., X_n)$$

when this limit exists, with H denoting the usual multivariate entropy of X, $H(X) = -E_X[\log(P(X)]$ [13, 19]. It is known that for a stochastic stationary processes,

$$\mathcal{H}(X) = \lim_{n\to\infty} H(X_n | X_{n-1}, X_{n-2} ..., X_1)$$

We note that entropy rate of a stochastic processes is non-increasing as a function of order, that is, $0 \leq \mathcal{H} \leq .. \leq H_q \leq ... \leq H_0 \leq 1$. A fundamental relation is that description length computed from LZW is closely related to entropy rate,

$$l_{LZW} = c(n) \log_2 [c(n) + \log_2 A] \approx c(n) \log_2 [c(n)] \longrightarrow n\mathcal{H}$$

The description length of the sequence encoded by LZW is the number of phrases times the number of bits needed to identify a seen phrase plus the bits to specify a new symbol (to form a new phrase), hence

$$l_{LZW} = c(n) \log_2 [c(n) + \log_2 A] \approx c(n) \log_2 [c(n)]$$

A reasonable strategy is to preserve as much information as possible in the resulting transformed string. In this sense, using methods that maximize the entropy of the resulting series are recommended, such as using the median for thresholding (this is guaranteed to result in $H_0 = 1$).

Two metrics are mainly used in the field: $c(n)$ and l_{LZW}. Of the two the latter is more closely related to Kolmogorov complexity or description length. Both contain similar information (in fact one is a monotonic function of the other). A natural way to normalize this metric is to divide description length by the original string length n

$$\rho_0 = l_{LZW}/n = \frac{c(n) \log_2[c(n) + A]}{n} \longrightarrow \mathcal{H}$$

with units of bits per character. This is the LZW compression ratio we will use here.

2.4. Data analysis

From the EEG data referenced to central electrodes we have generated a spectrogram stack of "frames" (time frequency bi-dimensional arrays) for each subject. To create it, EEG data for each channel was processed using Fourier analysis (FFT) after detrending one-second data blocks with a Hamming window (FFT resolution is 2 Hz). Each spectrogram frame was generated from 20 second long artifact free sequences from 14 EEG channel. Each frame was produced using a sliding window of one second. FFT amplitude bins in the band 4-44 Hz were used to ensure artifact-free frames. The FFT amplitudes were normalized by the sum in the 20–40 Hz band at each time step to reduce high frequency artifacts The resulting data frames are thus tensors of the form [channels (14)] x [FFTbins (21)] x [Epochs (20)].

Using this spectrogram frame dataset we carried out an analysis of the complexity of the frame subject datasets. For this purpose, the frame data for each subject was "flattened", that is, the tensor was converted to a one-dimensional array maintaining temporal adjacency in each frame (with flattening in this order: time in each frame, epoch, channel, frequency). The spectrogram hypercube flattened arrays for each subject were then been binarized using the median as a threshold. We computed ρ_0 and the entropy rate for orders 0 (H_0) to 5 (there are 2^6 =64 cases or "bins"in the associated histogram), and computed the log-log line fit slope as an additional metric (rateslope). For details and code used to compute LZW complexity see [19]. Since these metrics can be sensitive to data string length, we chose a reasonable string length and fixed it for all subjects data prior compression (using the first N bits, with $N = 10^6$ as a reasonable tradeoff).

3. Results

Entropy rates as a function of order are shown in Fig 1, displaying a linear decay in a log-log plot (a power law behavior). Complexity metrics per subject are shown, sorted, in Fig 2 together with the fast-to-slow ratio, and summarized in 3. In terms of statistical performance, using median binarization results in similar significance results for the relevant metrics (ρ_0, entropy rate and loglog entropy rate slope). Statistical results are summarized in Table 2 and Table 3. We note in passing that using mean instead of median binarization we obtained very similar results using the entropy rate log-log slope only.

We have also computed the fast-to-slow ratio as a metric using the same data, in this case as the ratio of power at frequencies 10-32 Hz (fast) versus 4 to 8 Hz (slow). This is essentially the same metric as proposed in [5]. The only differences are that we use the inverse (for plotting and discussion convenience), and that we are limited to frequencies larger than 4 Hz in our dataset.

We have seen here that RBD patients who later developed PD or DLB display diminished complexity in the spectrograms generated by EEG data com-

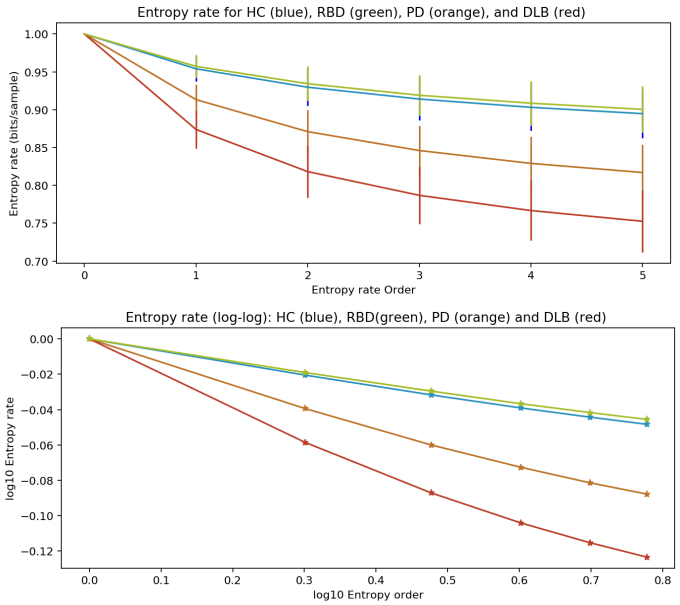


```
Entropy rate(order) Log-log plot linefit:
     HC  lineregress:  slope:-0.06 +- 0.01, r: -0.49, pval: 8.7e-25
     RBD lineregress:  slope:-0.06 +- 0.00, r: -0.49, pval: 7.0e-32
     PD  lineregress:  slope:-0.12 +- 0.02, r: -0.65, pval: 1.5e-10
     DLB lineregress:  slope:-0.16 +- 0.02, r: -0.70, pval: 1.4e-12
```

Figure 1: **Entropy rate as a function of order.** Top: entropy rate plot with error bar (standard error of the mean). Middle: log-log plot of the mean entropy rate. Bottom: refers to the line fit of subject data (after taking the logarithm of both axes).

pared to HCs or RBD patients who remained disease-free. The results of our statistical analysis are quite compelling, displaying very significant differences across two main super-groups: HCs and RBDs vs. PDs and DLBs. Data from the latter group display lower complexity and entropy rates. LZW and entropy rate provide essentially equivalent results.

These differences are remarkable as they reflect brain state at the moment of RBD diagnosis, years before conversion to PD or DLB. The performance of these metrics is slightly superior and complementary to those from power analysis [4, 5], to which they are well aligned.

Table 2: Mean complexity and fast-to-slow metrics for each group, with standard error of the mean (SEM).

Group (N)	ρ_0	H_5	fast-to-slow
HC (66)	1.05± 0.14	0.89 ± 0.01	2.28 ± 0.09
RBD (86)	1.06 ± 0.03	0.90 ± 0.02	2.10 ± 0.18
PD (13)	0.94 ±0.03	0.82 ± 0.02	1.71 ± 0.13
DLB (13)	0.85 ± 0.04	0.75± 0.03	1.44 ± 0.11

Table 3: Statistics for comparisons between groups: p-value (in scientific notation) and Area Under the Curve (AUC, in parenthesis). In the last row the Kruskal-Wallis p-value for the four groups is provided.

Comparison	ρ_0	H_5	fast-to-slow
HC vs. RBD	5×10^{-1} (53%)	6×10^{-1} (53%)	2×10^{-1} (57%)
HC vs. PD	4×10^{-3} (75%)	4×10^{-3} (75%)	4×10^{-3} (75%)
HC vs. DLB	7×10^{-5} **(85%)**	4×10^{-5} **(86%)**	3×10^{-5} **(87%)**
RBD vs. PD	3×10^{-3} (75%)	3×10^{-3} (75%)	4×10^{-2} (67%)
RBD vs. DLB	1×10^{-5} **(88%)**	1×10^{-5} **(88%)**	4×10^{-5} **(81%)**
PD vs. DLB	1×10^{-1} (67%)	1×10^{-1} (67%)	2×10^{-1} (64%)
HC vs. PD+DLB	7×10^{-6} **(80%)**	5×10^{-6} **(81%)**	3×10^{-6} **(81%)**
HC vs. rest	3×10^{-1} (55%)	3×10^{-1} (55%)	6×10^{-3} (62%)
HC+RBD vs. PD+DLB	4×10^{-7} **(81%)**	4×10^{-7} **(81%)**	1×10^{-5} (77%)
RBD vs. PD+DLB	1×10^{-6} **(82%)**	1×10^{-6} **(82%)**	2×10^{-4} (74%)
Kruskal-Wallis p-value	6×10^{-6}	5×10^{-6}	4×10^{-5}

4. Discussion

These results are in line with [3], where we hypothesized that while a brain capable of universal computation may produce many different types of patterns, both simple (e.g., constant or repetitive) and complex, a healthy brain engaging in modeling and prediction of complex I/Os will produce complex-looking, highly entropic data. Such apparent complexity is what is sequentially measured by entropy rate and LZW compression of electrophysiological or metabolic brain data [20, 21, 22, 23, 24]. First order entropy, entropy rate or LZW provide *upper bounds* on the algorithmic complexity of such data.

We note that although our full-band spectrogram complexity metrics were slightly more powerful in separating groups than the power ratio between high and low frequencies (fast-to-slow, see Table 3), they were correlated with power metrics (r$\sim$ 0.6, see Fig 2, bottom), a phenomenon already observed in previous studies in patients with neurodegenerative diseases [10, 12, 25]. The correlation of power metrics such as fast-to-slow ratio and LZW or entropic complexity is not entirely surprising. First, our complexity analysis was based on compression of spectrograms, and EEG power imbalances can be seen to lead to more compressible spectrograms after binarization. However, in addition to improving statistical separability, we note that complexity provides a rather general detection mechanism of regularities in the data. For example, imbalances in power ratio across arbitrary different bands may presumably lead to lower complexity after data binarization. But complexity metrics can detect such regularities in the data without the need to define a priori which specific aspects to use (e.g., which bands to use for a ratio computation). In this sense, they provide a rather assumption-free analysis of the data.

On the other hand, LZW and entropy rate can be sensitive to data flattening (that is, how multidimensional arrays are flattened into a one dimensional string). Here we have focused on the search for temporal patterns, as others using LZW in past work have. We have also seen that as expected, LZW and

entropy rate provide very similar metrics. LZW is much faster to compute, however.

Once complexity metrics detect differences across groups, it is interesting to investigate where specifically the changes in regularity lie in the data. In the case analyzed here, we carried out tests to find out, reordering and randomizing the data in different ways to see which led to loss of discrimination using power ratio or complexity features. In particular, we randomized the frequency index at each time point in each frame and channel independently. This shuffling destroyed the performance of both complexity and power ratio metrics. However, if the frequency randomization was held constant within each frame (but randomized across channels and frames), only the performance of the power ratio metric was severely affected (all suffered). Doing the same across the temporal dimension (reshuffling time in frames), which does not affect average power ratio metrics, increased complexity but did not affect discriminability of complexity metrics. Thus, complexity metrics appear to pick on the temporal variability of spectra in this dataset, which was highest for HC, then RBD, PD and DLB—irrespective of the actual shape of the spectrum. Poor prognosis in RBD appears to be associated with decreased temporal variability of the EEG spectrum.

Finally, we also investigated the role of high versus low frequency bands in these changes in complexity. Shortly, if only low frequency spectrogram data (below 10 Hz) was used to produce binarized strings, complexity metrics could not discriminate across classes. Instead, if only high frequency data was used, their performance was maintained ($f > 12$ Hz) or even increased ($f > 14$ Hz) with respect to the full-band case. The results are can be related to those in [25], where multiscale entropy was employed as complexity metric to study the differences in brain signal variability in PD patients who developed dementia at follow-up with respect who did not. They found significant changes, with lower signal variability at timescales sensitive to higher frequencies and higher signal variability for timescales sensitive to lower frequencies. We do note, however, that multiscale entropy and LZW (or entropy rate) measure complexity in slightly different ways.

We conclude that LZW and, equivalently, entropy rate highlight losses of complexity in spectrograms of PD or LBD patients at beta and gamma frequencies. Complexity scores in this band display much lower correlation with fast-to-slow metrics (r$\sim$0.3), indicating that they indeed provide complementary information to such spectral time averages.

Disclousure

Starlab and Neuroelectrics authors have an interest in developing commercial, translational applications from this research. GR is a shareholder of both companies.

Author contributions

DI pre-processed EEG data to produce artifact free spectrograms. EK and ASF contributed to code development and revised the manuscript. JFG, RP and JM collected the EEG data and revised the manuscript. GR provided the complexity analysis code, carried out the complexity and statistical analysis and wrote the manuscript.

Acknowledgments

This work partly supported by the Michael J. Fox Foundation within the project "Discovery of EEG biomarkers for Parkinson Disease and Lewy Body Dementia using advanced Machine Learning techniques" (Rapid Response Innovation Awards 2013), the FET Open Luminous project (H2020-FETOPEN-2014- 2015-RIA under agreement No. 686764) as part of the European Union's Horizon 2020 research and training programme 2014-2018, the Canadian Institutes of Health Research (CIHR) and the W. Garfield Weston Foundation.

References

[1] A. Soria-Frisch, J. Marin, D. I. Ibañez, S. Dunne, C. Grau, G. Ruffini, J. Rodrigues-Brazète, R. Postuma, J.-F. Gagnon, J. Montplaisir, A. Pascual-Leone, Machine learning for a Parkinson's prognosis and diagnosis system based on EEG., Proc. International Pharmaco-EEG Society Meeting PEG 2014, Leipzig, Germany.

[2] A. Soria-Frisch, J. Marin, D. Ibañez, S. Dunne, C. Grau, G. Ruffini, J. Rodrigues-Brazète, R. Postuma, J.-F. Gagnon, J. Montplaisir, A. Pascual-Leone, Evaluation of EEG biomarkers for Parkinson disease and other Lewy Body diseases based on the use of machine learning techniques, in preparation.

[3] G. Ruffini, An algorithmic information theory of consciousness, Neuroscience of Consciousness 3 (1).

[4] J. Rodrigues-Brazète, J. Gagnon, R. Postuma, J. Bertrand, M. J. D Petit, Electroencephalogram slowing predicts neurodegeneration in rapid eye movement sleep behavior disorder, Neurobiol Aging 37 (74-81).

[5] V. Latreille, J. Carrier, B. Gaudet-Fex, J. Rodrigues-Brazete, M. Panisset, S. Chouinard, R. B. Postuma, J.-F. Gagnon, Electroencephalographic prodromal markers of dementia across conscious states in Parkinson's disease, Brain 138 (2016) 1189–1199.

[6] L. Fantini, J. Gagnon, D. Petit, S. Rompre, A. Decary, J. Carrier, J. Montplaisir, Slowing of electroencephalogram in rapid eye movement sleep behavior disorder., Annals of neurology 53 (6) (2003) 774–780.

[7] A. Iranzo, A. Fernández-Arcos, E. Tolosa, M. Serradell, J. L. Molinuevo, F. Valldeoriola, E. Gelpi, I. Vilaseca, R. Sánchez-Valle, A. Lladó, C. Gaig, J. S. a, Neurodegenerative disorder risk in idiopathic REM sleep behavior disorder: Study in 174 patients, PLoS One 9 (2).

[8] S. Fulda, Idiopathic REM sleep behavior disorder as a long-term predictor of neurodegenerative disorders, EPMA J. 2 (4) (2011) 451–458.

[9] R. Postuma, J. Gagnon, M. Vendette, M. Fantini, J. Massicotte-Marquez, et al., Quantifying the risk of neurodegenerative disease in idiopathic REM sleep behavior disorder, Neurology 72 (2009) 1296–1300.

[10] C. Gomez, R. Hornero, D. Abasolo, M. Lopez, A. Fernandez, Decreased Lempel-Ziv complexity in Alzheimer's disease patients' magnetoencephalograms, Conf Proc IEEE Eng Med Biol Soc 5 (2005) 4514–7.

[11] D. Abásolo, R. Horner, C. Gómez, M. García, M. López, Analysis of EEG background activity in Alzheimer's disease patients with Lempel-Ziv complexity and central tendency measure, Medical Engineering & Physics 28 (4) (2006) 315–322.

[12] J. Dauwels, K. Srinivasan, M. R. Reddy, T. Musha, F.-B. Vialatte, C. Latchoumane, J. Jeong, A. Cichocki, Slowing and loss of complexity in Alzheimer's EEG: Two sides of the same coin?, International Journal of Alzheimer's Disease 2011 (Article ID 539621).

[13] T. M. Cover, J. A. Thomas, Elements of information theory, 2nd Edition, John Wiley & sons, 2006.

[14] M. Li, P. Vitanyi, An Introduction to Kolmogorov Complexity and Its Applications, Spriger Verlag, 2008.

[15] G. Ruffini, Models, networks and algorithmic complexity, Starlab Technical Note - arXiv:1612.05627 TN00339 (DOI: 10.13140/RG.2.2.19510.50249).

[16] A. Lempel, J. Ziv, On the complexity of finite sequences, IEEE Transactions on Information Theory IT-22 (1) (1976) 75–81.

[17] F. Kaspar, H. G. Schuster, Easily calculable measure for the complexity of spatiotemporal patterns, Phys. Rev. A 36 (2) (1987) 842–848.

[18] G. Ruffini, D. Ibañez, M. Castellano, S. Dunne, A. Soria-Frisch, EEG-driven RNN classification for prognosis of neurodegeneration in at-risk patients, ICANN 2016.

[19] G. Ruffini, Lempel-Ziv complexity reference, arXiv:1707.09848 [cs.IT].

[20] A. G. Casali, O. Gosseries, M. Rosanova, M. Boly, S. Sarasso, K. R. Casali, S. Casarotto, M.-A. Bruno, S. Laureys, G. Tononi, M. Massimini, A theoretically based index of consciousness independent of sensory processing and behavior, Sci Transl Med 5 (198).

[21] M. Schartner, A. Seth, Q. Noirhomme, M. Boly, M.-A. Bruno, S. Laureys, et al., Complexity of multi-dimensional spontaneous EEG decreases during propofol induced general anaesthesia, PLoS ONE 10 (8).

[22] T. Andrillon, A. T. Poulsen, L. K. Hansen, D. Leger, S. Kouider, Neural markers of responsiveness to the environment in human sleep, The Journal of Neuroscience 36 (24) (2016) 6583– 6596.

[23] A. G. Hudetz, X. Liu, S. Pillay, M. Boly, G. Tononi, Propofol anesthesia reduces Lempel-Ziv complexity of spontaneous brain activity in rats, Neurosci Lett. 628 (2016) 132–135.

[24] M. M. Schartner, R. L. Carhart-Harris, A. B. Barrett, A. K. Seth, S. D. Muthukumaraswamy, Increased spontaneous MEG signal diversity for psychoactive doses of ketamine, lsd and psilocybin, Scientific Reports 7 (46421).

[25] J.-A. Bertrand, A. McIntosh, R. Postuma, N. Kovacevic, V. Latreille, M. Panisset, S. Chouinard, J. Gagnon, Brain connectivity alterations are associated with the development of dementia in Parkinson's disease, Brain Connectivitry 6 (3) (2016) 216–224.

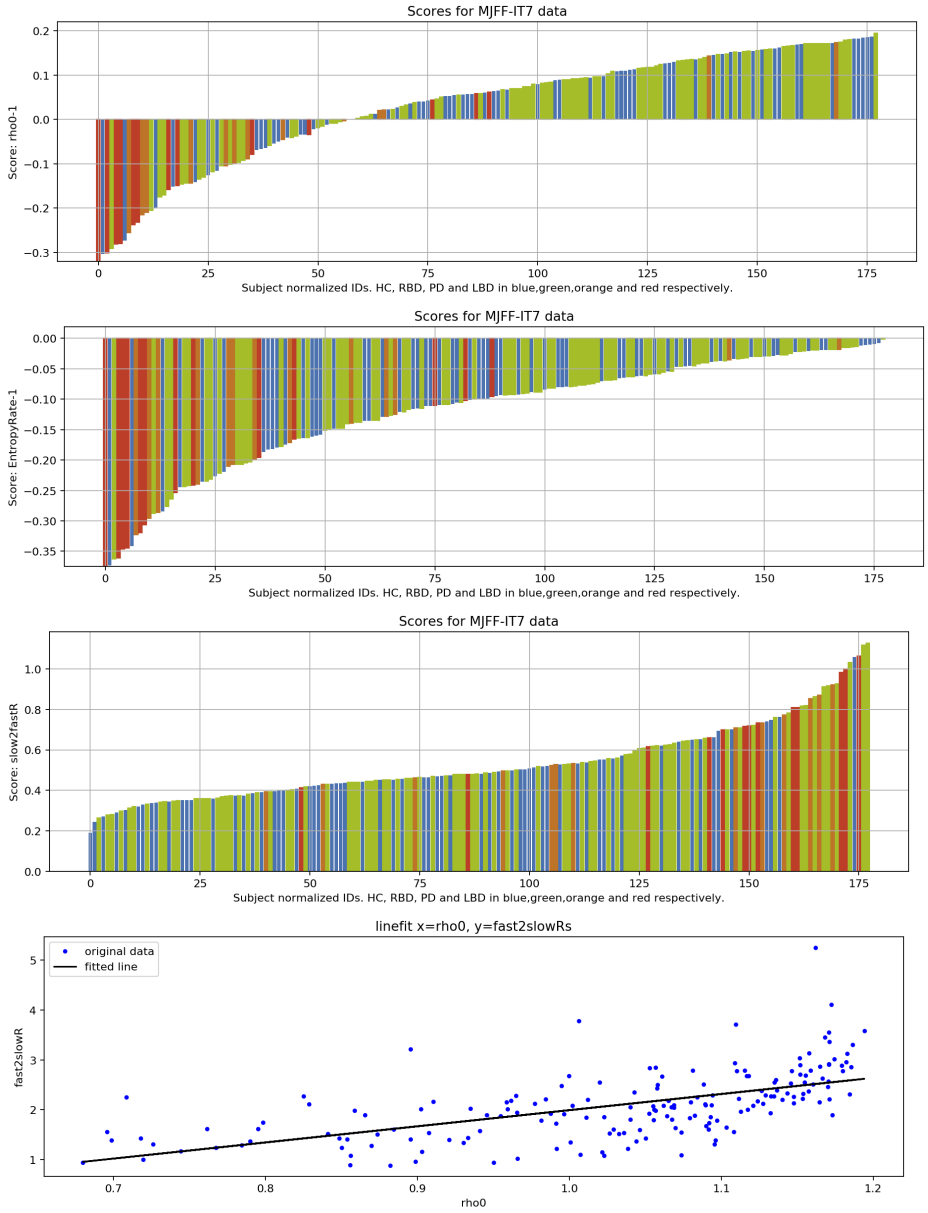

Figure 2: **Complexity, entropy rate and fast-to-slow scores per subject.** Complexity metric $\rho_0 - 1$ per subject for each class (HCs (66) in blue, RBDs (86) in green, PDs (13) in orange and DLBs (13) in red). The second plot displays "entropy rate-1" (i.e., $H_5 - 1$). The third one displays the fast-to-slow metric and the last displays ρ_0 vs fast-to-slow (line fit: slope: 3.2 ± 0.3, r: 0.60, pval: 1e-18).

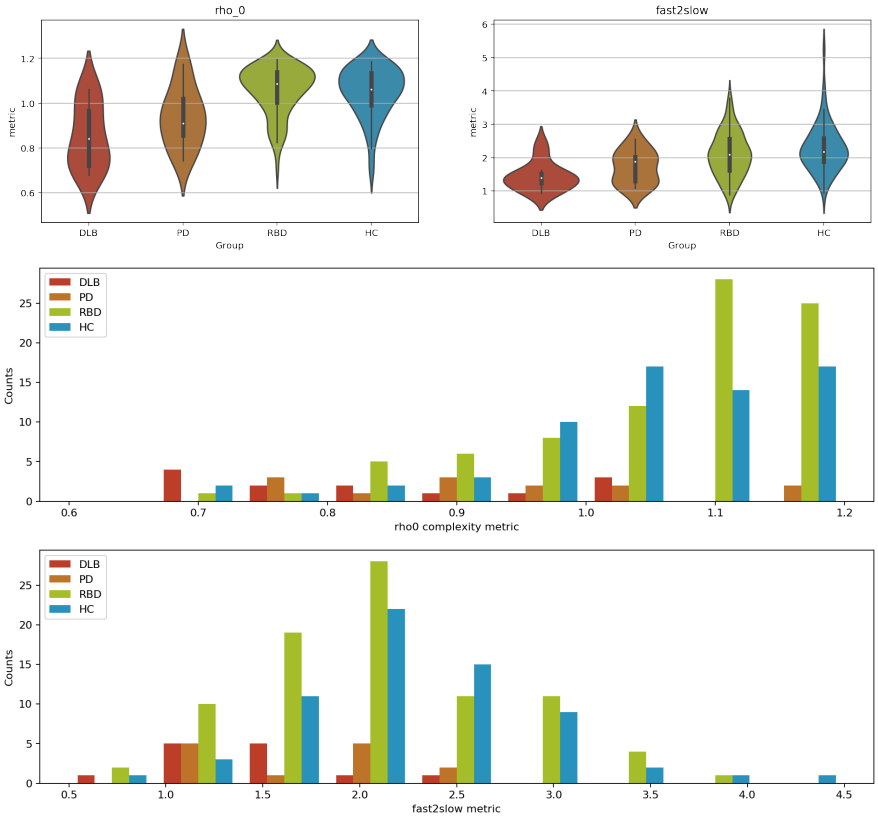

Figure 3: **Histograms and violin plots for ρ_0 complexity and fast-to-slow metrics.** Violin plots (with median) (top), and histograms for ρ_0 and fast-to-slow with each class (HCs (66) in blue, RBDs (86) in green, PDs (13) in orange and DLBs (13) in red).